P H Y S I C A L R E V I E W L E T T E R S

Transition to a Virtually Incompressible Oxide Phase at a Shock Pressure of 120 GPa (1.2 Mbar): Gd$_3$Ga$_5$O$_{12}$

T. Mashimo,[1] R. Chau,[2] Y. Zhang,[1] T. Kobayoshi,[3] T. Sekine,[3] K. Fukuoka,[4] Y. Syono,[4] M. Kodama,[5] and W. J. Nellis[6]

[1]*Shock Wave and Condensed Matter Research Center, Kumamoto University, Kumamoto 860-8555, Japan*
[2]*Lawrence Livermore National Laboratory, Livermore, California 94550, USA*
[3]*National Institute for Materials Science, Tsukuba 305-0044, Japan*
[4]*Institute for Materials Research, Tohoku University, Sendai 980-8577, Japan*
[5]*Sojo University, Kumamoto 860-0082, Japan*
[6]*Department of Physics, Harvard University, Cambridge, Massachusetts 02138, USA*
(Received 3 January 2006; published 17 March 2006)

Cubic, single-crystal, transparent Gd$_3$Ga$_5$O$_{12}$ has a density of 7.10 g/cm^3, a Hugoniot elastic limit of 30 GPa, and undergoes a continuous phase transition from 65 GPa to a quasi-incompressible (QI) phase at 120 GPa. Only diamond has a larger Hugoniot elastic limit. The QI phase of Gd$_3$Ga$_5$O$_{12}$ is more incompressible than diamond from 170 to 260 GPa. Electrical conductivity measurements indicate the QI phase has a band gap of 3.1 eV. Gd$_3$Ga$_5$O$_{12}$ can be used to obtain substantially higher pressures and lower temperatures in metallic fluid hydrogen than was achieved previously by shock reverberation between Al$_2$O$_3$ disks.

PACS numbers: 62.50.+p, 64.30.+t

Dynamic compression achieves pressures, densities, and temperatures that enable investigation of ultracondensed matter at conditions yet to be achieved by any other technique. The prototypical example is observation of minimum metallic conductivity (MMC) of dense fluid hydrogen at 140 GPa, ninefold compression of liquid density, and ~3000 K [1–3]. The high pressure and density and relatively low temperature are achieved by multiple-shock compression [2]. Temperature T is relatively low in the sense that $T/T_F \sim 0.01$, where T_F is the Fermi temperature. The time scale of compression is sufficiently long to achieve thermal equilibrium and sufficiently short so the process is adiabatic. Similar results are obtained for oxygen [4] and nitrogen [5]. Fluid Cs and Rb undergo the same transition at 2000 K near their liquid-vapor critical points [6]. All five elemental fluids have essentially the same value of MMC, and the density dependences of their semiconductivities scale with the quantum-mechanical charge-density distributions of the respective atoms [5]. Liquid H$_2$ is one of the most compressible of all materials.

In this Letter, we report that the dielectric crystal Gd$_3$Ga$_5$O$_{12}$ (GGG) transitions to a virtually incompressible phase at 120 GPa shock pressure. Prior to this investigation, single-crystal diamond and Al$_2$O$_3$ (sapphire) were the least compressible dielectric crystals known at high shock pressures. Diamond has a very low shock compressibility, remains elastic up to a shock stress of 70 GPa [7], and retains its diamond structure to more than 600 GPa [8,9]. Sapphire is elastic up to ~20 GPa and has phase transitions at high shock pressures, but the accompanying changes in compressibility are relatively small [10–12]. Gd$_3$Ga$_5$O$_{12}$ is more incompressible than sapphire at virtually all shock pressures and is more incompressible than diamond above 170 GPa shock pressure. Below 120 GPa, shock heating of GGG is sufficiently small that its shock-

compression curve is essentially coincident with its 300-K isotherm, measured previously up to 84 GPa in a diamond-anvil cell (DAC) [13]. GGG will enable substantially higher pressures (~300 GPa) and lower temperatures (~1500 K) to be achieved in fluid metallic hydrogen than was achieved previously with shock reverberation between sapphire disks [2], and GGG has implications for a new class of oxides at high pressures.

This quest was determined by the hydrodynamics of shock propagation. In a single shock, incompressibility is related to shock impedance $Z = \rho_0 u_s = P/u_p$, where ρ_0 is initial mass density, u_s is shock velocity, P is pressure, and u_p is particle (mass) velocity behind the shock front. The locus of states achieved by a series of single-shock compressions is called the Hugoniot curve. Shock impedance is related to incompressibility λ defined as $\lambda = (dP/d\eta)_H$, where $\eta = \rho/\rho_0$ and the derivative is along the Hugoniot. The Hugoniot equations yield $(dP/d\eta)_H = (\rho_0 u_s^2/\eta^2)[(1+x)/(1-x)]$, where $x = (u_p/u_s)(du_s/du_p)$. Large incompressibility λ means $\rho_0 u_s = Z$ is large.

Shock compression causes temperature to increase. For a highly incompressible material, shock temperatures and thermal pressures are relatively small, which means the Hugoniot and 300-K isotherm are nearly coincident, such as for diamond [9]. However, shock heating might have an appreciable effect on compressibility and phase transitions. Oxides, such as polycrystalline RuO$_2$ up to 40 GPa at 300 K [14], undergo phase transitions at high static pressures, and those phases might have high shock velocities.

For these reasons, we have investigated the cubic garnet Gd$_3$Ga$_5$O$_{12}$ with a density twice that of diamond. Average densities were 7.099 ± 0.006 g/cm^3, as measured by the Archimedean method. Specimens were single-crystal, transparent, cylindrical disks with a diameter of 13 or 18 mm and a thickness of about 2.4 mm obtained from

Princeton Scientific Corporation. Most specimens were oriented with their circular surfaces parallel to (111); a few had these surfaces parallel to (100). We measured equation-of-state data, dynamic strength, phase-transition pressures, and electrical conductivities of GGG single shocked in the range 30–260 GPa. Ultrasonic velocities were measured with the pulse-echo method. The tensor of elastic constants was determined by measuring longitudinal sound velocity c_L along $\langle 111 \rangle$, transverse velocity c_T along $\langle 100 \rangle$ and $\langle 111 \rangle$, and using the relation for elastic constants of a cubic crystal. Values of c_L along $\langle 100 \rangle$ and $\langle 111 \rangle$ were 6.557 and 6.433 km/s, respectively. Bulk and transverse sound velocities, c_B and c_T, were 5.107 and 3.458 km/s, respectively, about half those of diamond. Sound velocities were measured to within 0.1%.

Shock-wave profiles were measured with impactors accelerated up to 2, 4, and 6 km/s at Kumamoto University [15], Tohoku University [16], and the National Institute for Materials Science in Tsukuba [17], respectively, using the inclined-mirror technique. A streak camera record was published previously [18]. The 300-K isotherm was reduced from the Hugoniot using thermal corrections calculated with the Debye model and the Mie-Grüneisen equation of state [19]. Electrical conductivities [20] and shock-wave profiles with a velocity interferometer for a surface of any reflector (VISAR) [20] were measured at Lawrence Livermore National Laboratory.

Measured u_s-u_p data are plotted in Fig. 1. An unusually large increase in the slope of u_s is apparent at $u_p = 2.32$ km/s, indicative of a phase transition. These data were transformed to shock pressure P and density ρ with the Rankine-Hugoniot equations and plotted in Fig. 2. GGG is elastic up to a stress σ_{HEL}, where HEL is the Hugoniot elastic limit [21], which depends weakly on orientation and impactor velocity u_I. Along $\langle 111 \rangle$, $\sigma_{HEL} = 33$ and 31 GPa at $u_p = 0.66$ and 0.62 km/s, respectively. Along $\langle 100 \rangle$, $\sigma_{HEL} = 29$ GPa at $u_p = 0.57$ in two cases. The large σ_{HEL} of GGG (30 GPa) is about twice that of other materials except diamond (70 GPa) and is caused by its large initial mass density and the rigid covalent bonding of Gd and Ga with oxygen atoms. For comparison, values of the σ_{HEL} of single-crystal Al_2O_3 are 15–21 GPa [10,22], 25 GPa for $\langle 110 \rangle$ single-crystal cubic ZrO_2 doped with Y_2O_3 [19], 14–17 GPa for polycrystalline Si_3N_4 [23,24], 17 GPa for polycrystalline B_4C [25,26], and 16–19 GPa for polycrystalline SiC [27].

The two-wave shock structure of GGG indicates an elastic and plastic wave in the garnet structure up to the onset of a phase transition (PT) at $u_p = 1.35$ km/s, 65 GPa, a calculated temperature of 680 K, and a calculated thermal pressure of 1.5 GPa. Because of the small thermal pressure, PT is probably the onset of the amorphous phase observed in a DAC at 74 GPa. Under shock compression with shear stress, lattice defects, and temperature (680 K), it is reasonable to expect that the onset of this transition would occur at a shock pressure of 65 GPa, less than the 74 GPa observed in the DAC data.
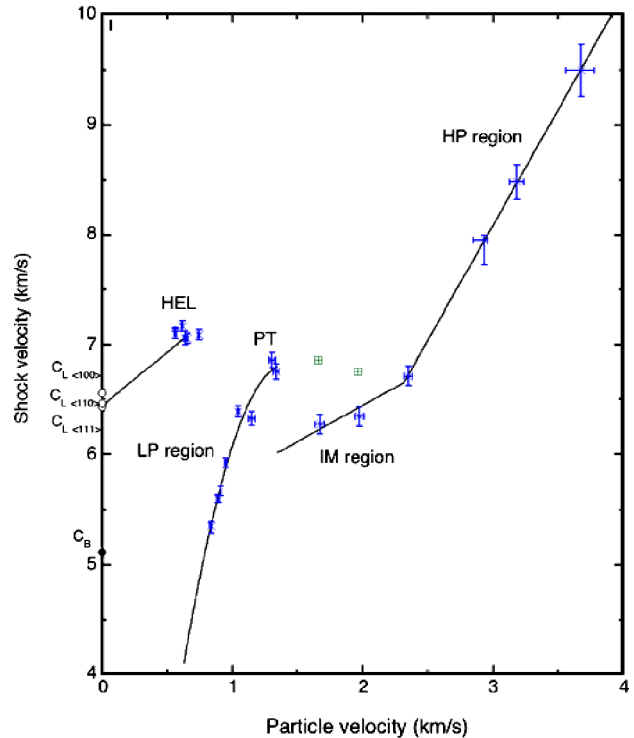

FIG. 1 (color online).   Shock velocity versus particle velocity of GGG: $\langle 111 \rangle$ direction (⊕), $\langle 100 \rangle$ direction (⊕), analyzed neglecting the small third wave in the IM phase (⊞). Shock velocity in the IM phase depends weakly on whether or not data analysis assumes phase transition occurs. HEL denotes Hugoniot elastic limit. PT denotes onset of continuous phase transition in the IM phase, which completes near $u_p = 2.3$ km/s at which GGG enters a virtually incompressible HP phase.

A small third wave was observed with the inclined mirror in the intermediate (IM) phase between PT and the onset of the high-pressure (HP) phase at $u_p = 2.32$ km/s and 120 GPa. The IM phase has strength and probably transforms continuously from the initial cubic structure at PT to the HP phase at 120 GPa that extends up to more than 260 GPa. The IM phase is probably the amorphous phase observed in a DAC [13], though its structure is yet to be determined. Since the static 300-K isotherm does not indicate a volume change at the onset of amorphization, any change in u_s at PT is expected to be small, as observed. VISAR data indicate the HEL and PT at particle velocities in good agreement with those measured with the inclined mirror. However, the third wave could not be observed with the VISAR because fringes were lost in the IM phase. Our diagnostic method is insensitive to strength in the HP phase. The u_s-u_p fits along $\langle 111 \rangle$ are $u_s = 6.433 + 0.98u_P$ for $0 < u_P < 0.67$ km/s, $u_s = -2.07 + 12.6u_p - 4.47u_p^2$ for $0.67 < u_p < 1.35$ km/s, $u_s = 5.13 + 0.66u_p$ for $1.35 < u_p < 2.32$ km/s, and $u_s = 1.79 + 2.10u_p$ for $2.32 < u_p < 3.70$ km/s.

The measured 300-K isotherm is plotted as P versus ρ [13] in Fig. 2. Those data show that GGG retains its low-pressure (LP) garnet phase up to 74 GPa. Diffraction lines
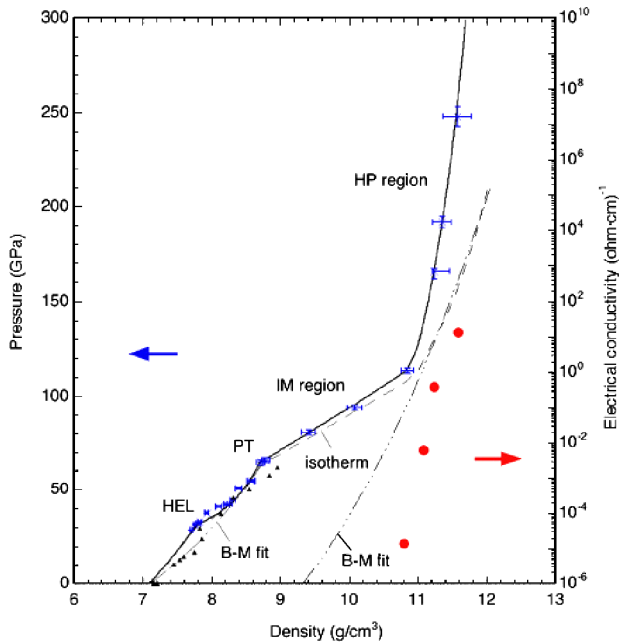
FIG. 2 (color online). Shock pressure and electrical conductivity of GGG versus shock density. Pressure is indicated on the left abscissa; electrical conductivity is indicated on the right abscissa: $\langle 111 \rangle$ direction ($\boxplus$), $\langle 100 \rangle$ direction ($\boxplus$), static 300-K isotherm ($\blacktriangle$) [13], electrical conductivity of $\langle 111 \rangle$ crystals ($\bullet$); B-M fits of HP and LP 300-K isotherms and a calculated 680-K isotherm in the IM phase are indicated. The diagnostic system to measure conductivity is insensitive to values less than 10^{-5} $(\Omega\,\text{cm})^{-1}$.

then broaden to 84 GPa; this line broadening was interpreted as amorphization. Under static compression, GGG remains transparent and electrically insulating to 90 GPa. Broadening of photoluminescence lines of GGG near 90 GPa was attributed to a change in site symmetry. Some silicates under static compression at 300 K become amorphous at pressures in which a continuous transition to a higher-pressure crystalline phase occurs. The DAC data suggest such a continuous transition begins at 74 GPa at 300 K.

Figure 2 shows that thermal pressure increases substantially in the HP phase, which is nearly incompressible. Thus, slope S of the HP phase is enhanced by shock temperatures and the associated increase in thermal pressures. At 250 GPa, $(dP/d\eta)_H$ is 2.4 and 0.89 TPa for GGG and diamond, respectively. In Fig. 3, P is plotted versus u_p for several dielectric crystals up to $\sim$300 GPa. Above 170 GPa, GGG has the highest shock impedance $Z = \rho_0 u_s = P/u_p$ and is less compressible than all of them, including diamond.

Electrical conductivities σ in Fig. 2 increase 6 orders of magnitude between 120 and 260 GPa shock pressure, which correlates well with completion of the transformation from the IM to the HP phase observed on the Hugoniot at 120 GPa. The calculated temperatures T of the HP phase increase from 1500 to 6500 K at pressures from 120 to
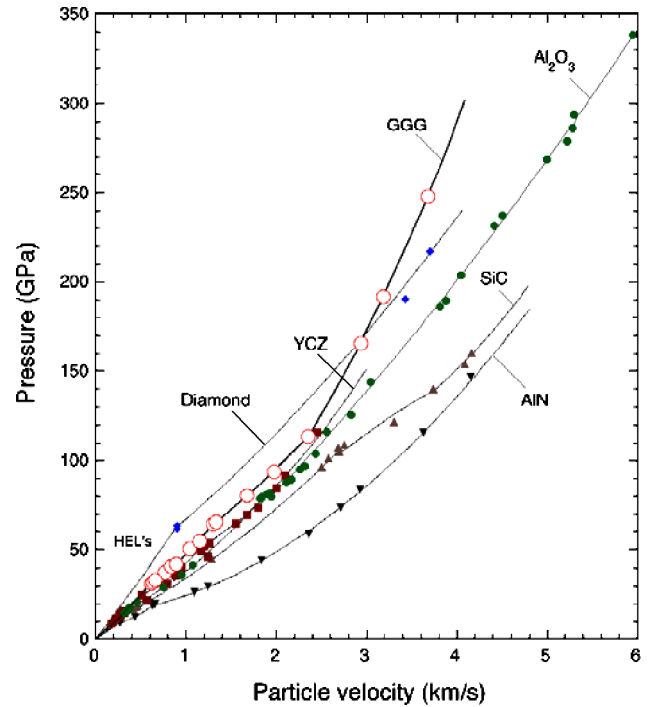

FIG. 3 (color online). Shock pressure versus particle velocity for several dielectric materials with high incompressibilities: GGG ($\bigcirc$), diamond ($\blacklozenge$), Al_2O_3 single crystals ($\bullet$), YCZ ($\blacksquare$), SiC ($\blacktriangle$), and AlN ($\blacktriangledown$).

250 GPa. Our measured conductivities fit $\sigma = \sigma_0 \exp(-E_g/2k_B T)$, where k_B is Boltzmann's constant, $\sigma_0 = 105$ $(\Omega\,\text{cm})^{-1}$, and $E_g = 3.1 \pm 0.1$ eV at 11.2 ± 0.4 g/cm^3. The facts that $\sigma_0 = 90$ $(\Omega\,\text{cm})^{-1}$ for fluid semiconducting hydrogen [2] and that the Hugoniot of graphite is less compressible than diamond and is probably in the fluid state above $\sim$200 GPa [9] suggest that the HP phase of GGG is a fluid. On the other hand, a band gap of 3.1 eV is intermediate between that of crystalline SiC (2.2–2.9 eV) and diamond (5.5 eV), which suggests that the HP phase might be an ordered solid.

Calculated 300-K isotherms of the LP and HP phases were obtained by correcting the Hugoniot for thermal pressure using the Debye and the Grüneisen models and fitting the Birch-Murnaghan (B-M) equation to the results in the LP and HP regimes. The density of the HP phase at $P = 0$ and 300 K derived from the fit is 9.32 ± 0.65 g/cm^3, a 30% increase over initial density of 7.10 g/cm^3. The bulk modulus K_0 of GGG derived from this fit is $K_0 = 440 \pm 6$ GPa ($K_0' = 4.8 \pm 0.3$), comparable to that of diamond.

Oxides with garnet structures are predicted to transform at high static pressures to a higher-coordination perovskite structure or to decompose (e.g., $2Gd_3Ga_5O_{12} \rightarrow 3Gd_2O_3 + 5Ga_2O_3$) [28]. The large volume collapse ($\sim$30%) is reasonable for a garnet to perovskite transition in GGG. However, because of the relatively short duration of shock experiments, the HP phase might have high local coordination typical of a dense perovskite phase and relatively

little long-range order because of the ~100 ns duration of the experiment. Since x-ray diffraction data are not available at high shock pressures, the structures of neither the HP nor the IM phase are yet known.

Collapse to a quasi-incompressible HP phase has not been observed in other oxides but might occur at sufficiently high pressures. The linear slope S of $u_s(u_p)$ in the IM phase of GGG is $S = 0.66$. Combining the Hugoniot equation $V = V_0(1 - (u_p/u_s))$ and the common relation $u_s = C + Su_p$, in the limit $C \ll Su_p$ limiting compression $(\rho/\rho_0)_L$ is simply related to the slope S: $(\rho/\rho_0)_L = S(S - 1) < 0$, which suggests that a phase transition must occur at sufficiently high pressure to a phase with a positive limiting compression. Limiting compression of the HP phase ($S = 2.1$) is 1.9. Since slope S of Al_2O_3 at highest pressures is 0.96, Al_2O_3 might also collapse to a substantially more incompressible phase above 340 GPa, the current maximum pressure of its Hugoniot measurements [12].

In summary, (i) GGG collapses to a quasi-incompressible phase at 120 GPa that is less compressible than diamond above 170 GPa shock pressure. This HP phase is a semiconductor with a band gap of 3.1 eV. (ii) The electrical conductivity of GGG remains less than $\sim100~(\Omega\,cm)^{-1}$ up to ~300 GPa. As a result, metal electrodes could be inserted through GGG disks to measure electrical conductivities of metallic fluid hydrogen [$\sim2000~(\Omega\,cm)^{-1}$] up to ~300 GPa using a reverberating shock wave. Thus, $Gd_3Ga_5O_{12}$ will enable achieving pressures and temperatures about 50% higher and lower, respectively, than was achieved previously in metallic fluid hydrogen by shock reverberation between Al_2O_3 disks [1–3]. (iii) It is possible that other oxides, such as Al_2O_3, undergo complete collapse to a quasi-incompressible phase at higher pressures than achieved thus far. (iv) Similar quasi-incompressible oxide phases composed of Si, Fe, Mg, and other elements with relatively high natural abundances, rather than Gd and Ga, might exist in the deep mantles of large extrasolar rocky planets [29].

[1] S. T. Weir, A. C. Mitchell, and W. J. Nellis, Phys. Rev. Lett. **76**, 1860 (1996).
[2] W. J. Nellis, S. T. Weir, and A. C. Mitchell, Phys. Rev. B **59**, 3434 (1999).
[3] V. E. Fortov, V. Ya. Ternovoi, S. V. Kvitov, V. B. Mintsev, D. N. Nikolaev, A. A. Pyalling, and A. S. Filimonov, JETP Lett. **69**, 926 (1999).
[4] M. Bastea, A. C. Mitchell, and W. J. Nellis, Phys. Rev. Lett. **86**, 3108 (2001).
[5] R. Chau, A. C. Mitchell, R. W. Minich, and W. J. Nellis, Phys. Rev. Lett. **90**, 245501 (2003).
[6] F. Hensel and P. Edwards, Phys. World **4**, 43 (1996).
[7] K. Kondo and T. J. Ahrens, Geophys. Res. Lett. **10**, 281 (1983).
[8] M. N. Palovskii, Sov. Phys. Solid State **13**, 741 (1971).
[9] W. J. Nellis, A. C. Mitchell, and A. K. McMahan, J. Appl. Phys. **90**, 696 (2001).
[10] T. Mashimo, K. Tsumoto, K. Nakamura, Y. Noguchi, K. Fukuoka, and Y. Syono, Geophys. Res. Lett. **27**, 2021 (2000).
[11] J. Lin, O. Degtyareva, C. T. Prewitt, P. Dera, N. Sata, E. Gregoryanz, H. K. Mao, and R. J. Hemley, Nat. Mater. **3**, 389 (2004).
[12] D. Erskine, in *High-Pressure Science and Technology–1993*, edited by S. C. Schmidt, J. W. Shaner, G. A. Samara, and M. Ross (AIP, New York, 1994), pp. 141–143.
[13] H. Hua, S. Mirov, and Y. K. Vohra, Phys. Rev. B **54**, 6200 (1996).
[14] J. Haines and J. M. Leger, Phys. Rev. B **48**, 13 344 (1993).
[15] T. Mashimo, S. Ozaki, and K. Nagayama, Rev. Sci. Instrum. **55**, 226 (1984).
[16] Y. Syono and T. Goto, Sci. Rep. Res. Inst. Tohoku Univ., Ser. A **29**, 17 (1980).
[17] T. Sekine, S. Tashiro, T. Kobayashi, and T. Matsumura, *Shock Compression of Condensed Matter–1995* (AIP, New York, 1996), p. 1201.
[18] Y. Zhang, T. Mashimo, K. Fukuoka, M. Kikuchi, T. Sekine, T. Kobayashi, R. Chau, and W. J. Nellis, in *Shock Compression of Condensed Matter–2003*, edited by M. D. Furnish, Y. M. Gupta, and J. W. Forbes (AIP, New York, 2004), pp. 127–128.
[19] T. Mashimo, A. Nakamura, K. Kodama, K. Kusaba, K. Fukuoka, and Y. Syono, J. Appl. Phys. **77**, 5060 (1995).
[20] L. M. Barker and R. E. Hollenbach, J. Appl. Phys. **43**, 4669 (1972); S. T. Weir, A. C. Mitchell, and W. J. Nellis, J. Appl. Phys. **80**, 1522 (1996).
[21] G. I. Kanel, S. V. Razorenov, and V. E. Fortov, *Shock-Wave Phenomena and the Properties of Condensed Matter* (Springer-Verlag, New York, 2004).
[22] R. A. Graham and W. P. Brooks, Phys. Chem. Solids **32**, 2311 (1971).
[23] A. Yamakawa, T. Nishioka, M. Miyake, K. Wakamori, A. Nakamura, and T. Mashimo, J. Ceram. Soc. Jpn. **101**, 1322 (1993).
[24] H. He, T. Sekine, T. Kobayashi, H. Horosaki, and I. Suzuki, Phys. Rev. B **62**, 11 412 (2000).
[25] M. E. Kipp and D. E. Grady, *Shock Compression of Condensed Matter–1989*, edited by S. C. Schmidt, J. N. Johnson, and L. W. Davison (North-Holland, Amsterdam, 1990), p. 377.
[26] T. Mashimo and M. Uchino, J. Appl. Phys. **81**, 7064 (1997).
[27] T. Sekine and T. Kobayashi, Phys. Rev. B **55**, 8034 (1997).
[28] N. Miyajima, K. Fujino, N. Funamori, T. Kondo, and T. Yagi, Phys. Earth Planet. Inter. **116**, 117 (1999).
[29] E. I. Rivera, J. J. Lissauer, R. P. Butler, G. W. Marcy, S. S. Vogt, D. A. Fisher, T. M. Brown, G. Laughlin, and G. W. Henry, Astrophys. J. **634**, 625 (2005).